BIOCHEMISTRY
including biophysical chemistry & molecular biology

Article

pubs.acs.org/biochemistry

Enzyme–Substrate Binding Kinetics Indicate That Photolyase Recognizes an Extrahelical Cyclobutane Thymidine Dimer

Johannes P. M. Schelvis,*[,†] Xuling Zhu,[‡,§] and Yvonne M. Gindt[†]

[†]Department of Chemistry and Biochemistry, Montclair State University, 1 Normal Avenue, Montclair, New Jersey 07043, United States

[‡]Department of Chemistry, New York University, 100 Washington Square East, New York, New York 10003, United States

ABSTRACT: *Escherichia coli* DNA photolyase is a DNA-repair enzyme that repairs cyclobutane pyrimidine dimers (CPDs) that are formed on DNA upon exposure of cells to ultraviolet light. The light-driven electron-transfer mechanism by which photolyase catalyzes the CPD monomerization after the enzyme–substrate complex has formed has been studied extensively. However, much less is understood about how photolyase recognizes CPDs on DNA. It has been clearly established that photolyase, like many other DNA-repair proteins, requires flipping of the CPD site into an extrahelical position. Photolyase is unique in that it requires the two dimerized pyrimidine bases to flip rather than just a single damaged base. In this paper, we perform direct measurements of photolyase binding to CPD-containing undecamer DNA that has been labeled with a fluorophore. We find that the association constant of ~2×10^6 M^{-1} is independent of the location of the CPD on the undecamer DNA. The binding kinetics of photolyase are best described by two rate constants. The slower rate constant is ~10^4 M^{-1} s^{-1} and is most likely due to steric interference of the fluorophore during the binding process. The faster rate constant is on the order of 2.5×10^5 M^{-1} s^{-1} and reflects the binding of photolyase to the CPD on the DNA. This result indicates that photolyase finds and binds to a CPD lesion 100–4000 times slower than other DNA-repair proteins. In light of the existing literature, we propose a mechanism in which photolyase recognizes a CPD that is flipped into an extrahelical position via a three-dimensional search.

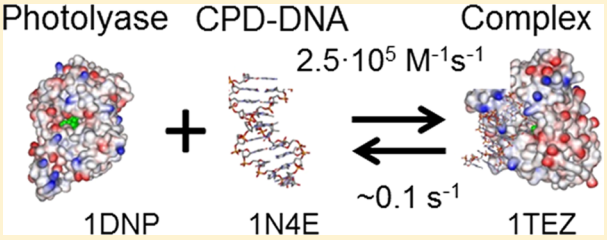

Photolyases are structure-specific DNA-repair enzymes that are found in all kingdoms of life except for placental mammals, and they repair DNA lesions that have been induced by ultraviolet (UV) light.[1−3] The most common photolyase repairs the major DNA UV photoproduct, the *cis,syn* cyclobutane pyrimidine dimer (*cs*CPD) that forms between adjacent pyrimidine bases.[1,4,5] The repair mechanism can be broken down into two separate but equally important steps. First, the enzyme searches for and binds to the damaged site on DNA. Second, once the enzyme–substrate complex has formed, the enzyme has to absorb a blue photon to initiate the catalytic cycle of *cs*CPD monomerization. While the mechanism by which DNA photolyase repairs CPD lesions after formation of the enzyme–substrate complex is relatively well understood,[1,6−8] the means by which the enzyme recognizes and binds to CPD lesions on DNA is still not clear.

The first X-ray crystal structure of DNA photolyase indicated that the active site flavin adenine dinucleotide (FAD) was located at the bottom of a cleft that was presumed to be the CPD binding site.[9] This structural evidence suggested that the CPD would have to assume an extrahelical position to bind to DNA photolyase. Subsequently, such a binding geometry was predicted by computer modeling and computational studies.[10−12] The first experimental evidence of extrahelical CPD–photolyase binding geometry came from the Stanley group,[13,14] and their interpretation was supported by subsequent nuclear magnetic resonance (NMR) and optical spectroscopy experiments.[15−18] A later X-ray crystal structure of photolyase complexed to CPD-containing DNA confirmed the extrahelical binding geometry, although the CPD appeared to have been repaired during the data collection process.[19] Photolyase clearly requires an extrahelical CPD binding geometry, but NMR solution and X-ray crystal structures of CPD-containing DNA show an intrahelical CPD;[20,21] therefore, the CPD has to flip out of the DNA helix for the formation of the enzyme–substrate complex. Although other DNA-repair proteins also require base flipping of the damaged site,[22,23] photolyase is unique because it requires two dimerized thymidines to flip out of the double helix rather than a single damaged base. The role of the enzyme in base flipping is not completely clear. A computational study of *cs*CPD-containing DNA and a recent isothermal calorimetry study of photolyase–substrate binding provided support for binding of photolyase to an extrahelical CPD that spontaneously flips out of the double helix.[24,25] However, a recent NMR study of base flipping in *cs*CPD-containing DNA argued against the spontaneous movement of the *cs*CPD into an extrahelical position as a viable mechanism.[26]

Over the past few decades, a general picture of how proteins search for and find a specific sequence or a specific site target

Received: August 19, 2015
Revised: September 14, 2015
Published: September 22, 2015

DOI: 10.1021/acs.biochem.5b00927
Biochemistry 2015, 54, 6176–6185

Table 1. Properties of the Oligonucleotides Used in This Study

oligonucleotide	sequence (5′ → 3′)[a]	molar extinction coefficient at 260 nm (M^{-1} cm^{-1}) without CPD[b]	molar extinction coefficient at 260 nm (M^{-1} cm^{-1}) with CPD[c]	molar extinction coefficient at 521 nm (M^{-1} cm^{-1}) with TET at the 5′-terminus[b]
Oligo1	GCA AG**T T**GG AG	113300	97900	
Oligo2	CGA **TT**G GAG AG	114400	99000	
Oligo3	**GTT** GGA GAG AC	114600	99200	
Complementary-1	CTC CAA CTT GC	93800		86000
Complementary-2	CTC TCC AAC TG	94900		86000
Complementary-3	GTC TCT CCA AC	96900		86000

[a]Position of T-T to form *cis,syn* CPD shown in bold. [b]Data from TriLink Technologies. [c]Calculated by using the nearest-neighbor model.[42]

on DNA has emerged.[27,28] First, the protein binds nonspecifically to the DNA with a diffusion-controlled rate constant. Then, the protein uses "facilitated diffusion" to locate its target sequence or site on the DNA. The facilitated diffusion can occur through sliding, hopping, or jumping to search for the target in a unidimensional way. During sliding, the protein fully remains in contact with the DNA, but it is only efficient over short distances, 10−50 bp.[27,28] During hopping (<10 bp) and jumping (>100 bp), the protein dissociates from the DNA molecule but remains in its vicinity because of electrostatic interactions and lands on a different part of the same DNA molecule. All three processes will compete with the complete dissociation of the protein from the DNA. From the literature, it appears that the proteins that follow this search mechanism bind to their target on the DNA with a binding rate constant ranging from 1.7×10^7 to 9.0×10^8 M^{-1} s^{-1},[29−34] including proteins that require base flipping as part of the search process.

Indirect determination of the binding rate constant of photolyase in *Escherichia coli* cells *in vivo* and with plasmid DNA *in vitro* gave rate constants of 1.1×10^6 and 4.2×10^6 M^{-1} s^{-1}, respectively, at room temperature.[35,36] These rate constants are 2−3 orders of magnitude slower than those reported for other site-specific DNA-repair enzymes[29−34] and hint that the DNA damage recognition and binding process is quite different and potentially more complex for photolyase. Direct measurements of the kinetics of the formation of the enzyme−substrate complex are required to address this discrepancy.

In this work, we investigate the binding of photolyase to *cs*CPD-containing dsDNA as a function of CPD position on the DNA by using steady-state and stopped-flow fluorescence spectroscopy. The DNA is tagged with a fluorophore, tetrachlorofluorescein (TET), and *E. coli* photolyase is used in its purified form with the flavin cofactor present as the neutral radical semiquinone ($FADH^•$).[37] Under these conditions, the binding of photolyase to *cs*CPD-DNA can be directly monitored by the quenching of the TET excited state via Förster resonance energy transfer (RET) to the $FADH^•$ in photolyase. Förster RET between two chromophores has three main requirements: the donor−acceptor distance should be <60 Å, the overlap integral has to be non-zero, and the transition dipole moments have to be properly oriented with respect to each other.[38,39] Our donor (TET)−acceptor ($FADH^•$) pair fulfills these requirements. First, the *cs*CPD binds close to the FAD cofactor,[19] with an estimated maximal distance between TET and $FADH^•$ of 32 Å, the length of the undecamer dsDNA used in this study. Second, the TET emission ranges from 530 to 590 nm, while $FADH^•$ in photolyase absorbs visible light from 450 to 650 nm. Therefore, the TET emission transition dipole moment and the $FADH^•$ absorption transition dipole moment resonate at similar frequencies, and the overlap integral for RET is non-zero. Finally, the linker that attaches TET to the DNA provides it with rotational freedom, which will allow its emission transition dipole moment to sample many different orientations with respect to the $FADH^•$ absorption transition dipole moment to support RET.

Our binding studies show that the location of the *cs*CPD, with one exception, on the undecamer dsDNA did not have much effect on either the equilibrium binding constant or the binding rate constant of DNA photolyase to the substrate. The differences that were observed in the binding rate constant can be explained by steric interference from the fluorophore. The implications of our findings for the mechanism of CPD recognition and binding by photolyase will be discussed.

MATERIALS AND METHODS

Materials. Oligonucleotides and their complementary strands with and without tetrachlorofluorescein (TET) attached at the 5′-terminus were purchased from TriLink Biotechnologies (see Table 1 for sequences). All the complementary oligonucleotides were purchased in high-performance liquid chromatography (HPLC)-purified form, and the oligonucleotides that were used for *cs*CPD formation were purchased in desalted form. All other chemicals were from Sigma-Aldrich.

Enzyme Preparation. *E. coli* strain pMS969 was a generous gift from A. Sancar. The cells were grown and harvested, and the enzyme was isolated and purified as described previously.[37] The purified enzyme in the semiquinone form was stored in 50 mM HEPES and 0.4 M K_2SO_4 (pH 7) at −80 °C until the enzyme was used. The enzyme concentration was determined by using an extinction coefficient at 580 nm of 4800 M^{-1} cm^{-1}.[40]

Preparation and Purification of *cs*CPD-Containing Oligonucleotides. We used a modified method from the literature for the preparation and purification of *cs*CPD-containing oligonucleotides.[41] Each oligonucleotide was dissolved in deionized, distilled water to a concentration of 150 μM in the presence of 20−40 mM acetophenone, which was used as a photosensitizing agent. The sample was placed in a semimicro quartz cuvette that was sealed with a septum and screw-cap. The samples were purged with nitrogen gas for 15 min and irradiated anaerobically on ice with a UV lamp (8 W, 302 nm, model UVM-28, UVP). The optimal irradiation time for *cs*CPD formation was 6 h for Oligo1 and Oligo3 and 4 h for Oligo2 as monitored by HPLC analysis. In the remainder of the paper, Oligo1, Oligo2, and Oligo3 refer to the strands containing the adjacent TT sequence for *cs*CPD formation as listed in Table 1 and DNA1, DNA2, and DNA3 refer to the

DOI: 10.1021/acs.biochem.5b00927
Biochemistry 2015, 54, 6176−6185

dsDNA formed between the specific oligonucleotides and their complementary strands. The prefix *cs*CPD indicates that the oligonucleotide or DNA contains a *cs*CPD lesion.

The UV-irradiated oligonucleotides were purified by reversed-phase HPLC, using a 250 mm × 4.6 mm Microsorb-MV C18 column (Varian) and a Jasco HPLC system consisting of two PU-987 intelligent prep. pumps, an HG 980-31 solvent mixer, and an MD-910 multiwavelength detector. The mobile phase was a mixture of acetonitrile (ACN) and 0.1 M triethylammonium acetate buffer at pH 7.0 (TEAA). For the *cs*CPD of Oligo1, the gradient was 7 to 12% (v/v) ACN over 25 min, followed by 12 to 70% (v/v) ACN over 5 min. The *cs*CPD of Oligo1 eluted after 16.8 min. For the *cs*CPD of Oligo2, the gradient was 8 to 10% (v/v) ACN over 15 min, followed by 10 to 12% (v/v) ACN over 10 min and 12 to 70% (v/v) ACN over 5 min. The *cs*CPD of Oligo2 eluted after 10 min. The gradient used to purify the *cs*CPD of Oligo3 was 8 to 10% (v/v) ACN over 5 min, followed by 10 to 12% (v/v) ACN over 10 min and 12 to 70% (v/v) ACN over 10 min. The *cs*CPD of Oligo3 eluted after 10.2 min. At the end of each HPLC run, the mobile phase was held at 70% (v/v) ACN until acetophenone had eluted. The mobile-phase flow rate was kept at 1.0 mL/min.

Purified oligonucleotides were concentrated, and ACN was removed using rotary evaporation. The oligonucleotides were desalted by equilibrating the HPLC column with deionized water for 20 min. The mobile phase consisted of deionized water for 10 min followed by 50% deionized water and 50% ACN for 20 min. The purified *cs*CPD oligonucleotides eluted between 17 and 19 min.

The concentration of each *cs*CPD oligonucleotide was determined from its absorption at 260 nm by using the extinction coefficients (Table 1) that were calculated from the nearest-neighbor method.[42] Because the *cs*CPD absorbs only weakly at 260 nm,[4] the extinction coefficient of the *cs*CPD oligonucleotides was determined by treating them as two separate oligonucleotides, one 5′ from the CPD and one 3′ from the CPD, and adding the calculated extinction coefficient of each segment.

The purity of the HPLC-purified oligonucleotides with and without the *cs*CPD was checked by sodium dodecyl sulfate−polyacrylamide gel electrophoresis and phosphorimaging, and the binding of photolyase to the *cs*CPD oligonucleotides was confirmed on a nondenaturing gel (data not shown).

Melting Temperature Measurements. Each oligonucleotide was mixed with an equimolar quantity of its complementary strand with or without the 5′-TET to a final concentration of 3 μM in cacodylate buffer [40 mM sodium cacodylate, 11 mM magnesium acetate, and 1 mM EDTA (pH 6.5)]. The sample was placed in a 95 °C water bath that was cooled slowly to room temperature overnight to anneal the complementary strands to form dsDNA. Up to six melting temperature experiments were performed simultaneously on a Cary 100 UV−vis absorption spectrophotometer. For each experiment, the temperature was changed between 15 and 75 °C at a heating/cooling rate of 0.3 °C/min. The derivative method was used to determine the melting temperature for each duplex, and replicate experiments were performed to obtain the average melting temperature.

Photolyase−DNA Binding Experiments. Binding constants for photolyase with each of the *cs*CPD-DNAs were determined at 15 °C by fluorescence intensity measurements on a fluorescence spectrophotometer (F-2500, Hitachi). The *cs*CPD oligonucleotides were combined with their 5′-TET-labeled complementary strands in a 1:1.4 ratio. The reaction mixture contained 0.5 nmol of dsDNA in 50 mM Hepes and 0.4 M K_2SO_4 (pH 7.0). The excitation wavelength was 525 nm, and the emission spectrum was measured from 530 to 620 nm. The excitation and emission bandwidths were 5 nm, and the scan speed was 300 nm/min. Small aliquots of DNA photolyase were added to the reaction mixture until the fluorescence intensity remained unchanged. Each titration was repeated at least three times. Control experiments were performed with undamaged dsDNA under identical conditions and did not show any significant change (data not shown). The titration data were fit to a one-binding site model to determine the association constant (Microcal Origin 7.0).

Fluorescence Stopped-Flow Experiments. The experiments were performed at 15 °C on a Hi-Tech Scientific DX 2 stopped-flow instrument. The excitation wavelength was 520 nm, and the emission light was passed through a 530 nm bandpass filter to block stray excitation light. The *cs*CPD-dsDNA (2 μM) was rapidly mixed with 20, 30, 40, 60, and 100 μM photolyase to final molar ratios of 1:10, 1:15, 1:20, 1:30, and 1:50, respectively. Each kinetic trace consisted of 2048 equally spaced data points, and multiple time courses (6−10 runs) ranging from 1 to 20 s with sampling intervals from 0.5 to 10 ms, respectively, were analyzed by fitting to mono- or biexponential decay curves (Microcal Origin 7.0). The reaction rates, the amplitudes, and the offset were freely adjustable fit parameters. Control experiments were conducted by mixing undamaged DNA with photolyase or buffer and damaged DNA with buffer, which resulted in no or insignificant increases in fluorescence intensity as opposed to a significant decrease in intensity that was observed when mixing damaged DNA and photolyase (data not shown).

RESULTS

Effect of CPD Location on Melting Temperature. The melting temperatures of the dsDNA constructs were determined by UV−vis absorbance spectroscopy, and typical melting curves are shown in Figure 1. The melting curves have been normalized to facilitate comparison to each other, and the melting temperatures are listed in Table 2. The melting temperature (T_m) ranged from 54 to 55 °C for the three DNA constructs without the *cs*CPD, while the T_m ranged from 46 to 47 °C for the corresponding DNA constructs with the *cs*CPD. The 7−8 °C decrease in melting temperature in the presence of the *cs*CPD is in good agreement with those of similar systems in the literature.[20,43−45]

As seen in Table 2, the presence of TET at the 5′-terminus of the complementary strand does not have a significant effect on the melting temperature of the DNA constructs; therefore, it has no significant effect on the thermal stability of these DNA constructs. The similarity in melting temperatures of the three different dsDNA constructs is not surprising because their GC content was kept the same and either terminus was capped with a GC base pair. From our results, it is also clear that the thermal stability of dsDNA is independent of the location of the *cs*CPD on the undecamer dsDNA.

Fluorescence Spectrophotometric Titration of *cs*CPD-dsDNA with Photolyase. The fluorescence emission spectrum of the complementary strand of Oligo1 with TET attached is shown in Figure 2A (solid line). When the *cs*CPD-Oligo1 is added to form *cs*CPD-DNA1, the TET fluorescence intensity decreases by 59% (Figure 2A, dashed line), which is

DOI: 10.1021/acs.biochem.5b00927
Biochemistry 2015, 54, 6176−6185

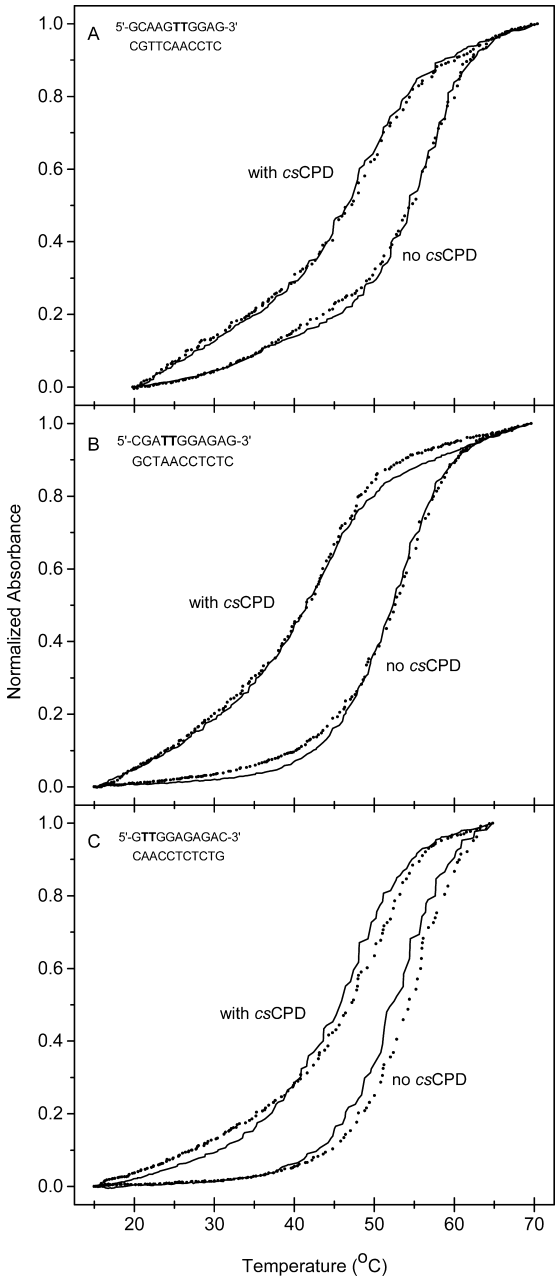

Figure 1. Absorbance-detected thermal denaturation curves of (A) DNA1, (B) DNA2, and (C) DNA3 in the absence (—) and presence (···) of the TET fluorophore and in the absence or presence of the *cs*CPD as indicated in the graph. The absorbance change of the denaturation curves has been normalized to facilitate comparison.

likely due to fluorescence quenching by the GC base pair adjacent to TET.[46] Addition of a 3-fold excess of photolyase to *cs*CPD-DNA1 causes an additional 13% decrease in TET fluorescence (Figure 2A, dotted line). This decrease in TET fluorescence is due to RET from TET to the $FADH^{\bullet}$ in photolyase, as described above.

The emission spectra for TET-labeled complementary strands of Oligo2 and Oligo3 are shown in panels B and C of Figure 2, respectively (solid lines). Upon addition of *cs*CPD-Oligo2 to form *cs*CPD-DNA2, the TET fluorescence decreases by 53% (Figure 2B, dashed line), and addition of a 3-fold molar excess of photolyase to *cs*CPD-DNA2 decreases the fluorescence by an additional 4% (Figure 2B, dotted line). In contrast, addition of *cs*CPD-Oligo3 to form *cs*CPD-DNA3 lowers the TET fluorescence by 10% (Figure 2C, dashed line), while addition of a 3-fold molar excess of photolyase to *cs*CPD-DNA3 decreases the fluorescence by an additional 10% (Figure 2C, dotted line).

Table 2. Melting Temperatures of the dsDNA Constructs Used in This Study

	melting temperature (°C)			
	T_T[b]		T<>T[c]	
sequence[a]	no TET	TET	no TET	TET
5′-GCAAGTTGGAG-3′ 3′-CGTTCAACCTC-5′	54 ± 1	55 ± 1	49 ± 1	48 ± 1
5′-CGATTGGAGAG-3′ 3′-GCTAACCTCTC-5′	53 ± 1	55 ± 1	44 ± 1	45 ± 1
5′-GTTGGAGAGAC-3′ 3′-CAACCTCTCTG-5′	53 ± 2	55 ± 1	48 ± 1	46 ± 1

[a]Position of *cis,syn* CPD shown as **TT**. [b]Undamaged DNA. [c]*cs*CPD-containing DNA.

Typical photolyase titration curves for each DNA construct are shown as insets in the respective graphs of Figure 2; the data are plotted with the inverse of the change in the emission to facilitate the data analysis. The titration curves were fit to a one-site binding model to determine the association constant for photolyase with each of the *cs*CPD-DNA constructs. The resulting association constants (K_A) of three to five replicate trials are listed in Table 3, with all values around 2×10^6 M^{-1}. These results show that neither the location of the *cs*CPD on these DNA constructs nor the presence of TET appears to significantly affect the association constant for association of photolyase with *cs*CPD-DNA.

Photolyase *cs*CPD-DNA Binding Kinetics Detected by Fluorescence Spectroscopy. Representative traces of the fluorescence stopped-flow experiments for the binding of photolyase to *cs*CPD-containing DNA are shown in Figure 3. Although only every other 25th data point (●) of each trace is shown to facilitate observation of the fits (—), the full data sets were used to fit the data. The kinetic traces that are obtained for *cs*CPD-DNA1 and *cs*CPD-DNA3 are best fit to a biexponential decay function. In the case of *cs*CPD-DNA1, the kinetics consist of a fast phase and a slow phase, which account for 65 and 35%, respectively, of the decay of the fluorescence intensity. In the case of *cs*CPD-DNA3, the fast phase is much more dominant and accounts for >85% of the decay of the fluorescence intensity. In contrast, the kinetic traces for *cs*CPD-DNA2 are best described by a monoexponential decay function with the rate of binding of photolyase to *cs*CPD-DNA2 found to be similar to that of the slow phase that is observed for *cs*CPD-DNA1 and *cs*CPD-DNA3. We did not find any evidence of faster kinetic signals. First, the percent change in fluorescence intensity was virtually unchanged: 25 ± 1% for DNA1 and 17 ± 1% for DNA3 at the various enzyme concentrations. Second, kinetic traces taken with a 1 s run time and 0.5 ms integration intervals and with a 10 s run time and 5 ms integration intervals are identical within the noise of the experiment. The insets in Figure 3 show the apparent rate constants plotted as a function of enzyme concentration (■) together with a linear fit (—). The rate constants for binding of photolyase to the three different *cs*CPD-containing DNAs are determined by the slope of the linear fit with assumption of first-order enzyme kinetics and shown in Table 3. The rate

DOI: 10.1021/acs.biochem.5b00927
Biochemistry 2015, 54, 6176−6185

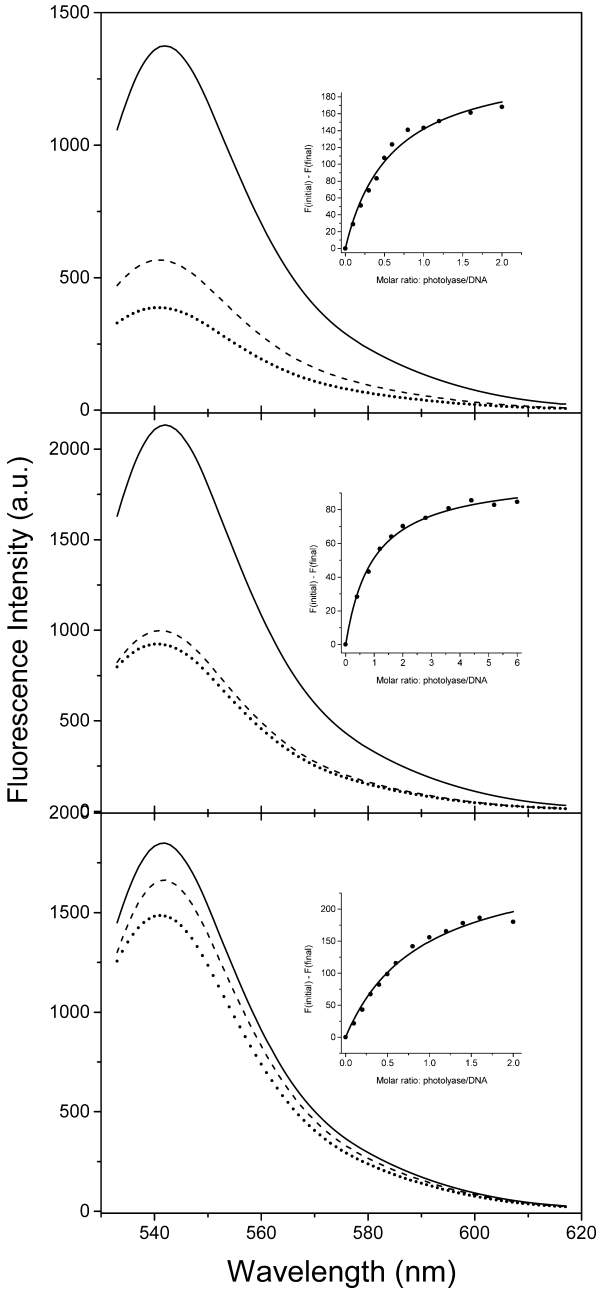

Figure 2. Fluorescence-detected binding of photolyase to *cs*CPD-containing DNA. Each graph shows the emission spectrum of the complementary strand with TET attached (—), of the complementary strand with TET and a 1.4-fold molar excess of *cs*CPD-containing oligonucleotide (---), and of the complementary strand with TET, a 1.4-fold molar excess of *cs*CPD-containing oligonucleotide, and a 6-fold molar excess of photolyase (···). Emission spectra are shown for (A) *cs*CPD-DNA1, (B) *cs*CPD-DNA2, and (C) *cs*CPD-DNA3. The inset of each graph shows the photolyase titration curve with the inverse change in emission intensity on the *y*-axis.

constants for binding of photolyase to *cs*CPD-DNA1 and *cs*CPD-DNA3 are very similar, ~2.5 × 10^5 M^{-1} s^{-1}, and the rate constant for binding to *cs*CPD-DNA2 is ~10 times slower, ~2.3 × 10^4 M^{-1} s^{-1}.

DISCUSSION

Influence of the Fluorophore and CPD on DNA Thermal Stability. The thermal stability of the *cs*CPD-DNAs was monitored by determining the melting temperature (T_m). Because the GC content was the same for all three DNA constructs, their melting temperatures were very similar, and the presence of the TET fluorophore at the 5′-terminus of the complementary strand did not change the T_m of the DNA constructs in a manner independent of the *cs*CPD. Thus, we conclude that the presence of TET does not alter the thermal stability of the dsDNA constructs with or without the *cs*CPD present in any significant way. The T_m of DNA1 is significantly higher (54 °C) than that reported in the literature (45 °C).[44] The higher T_m determined in our studies is most likely due to a higher oligonucleotide concentration (3.0 μM compared to 0.70 μM), though a difference in the ionic strength of the oligonucleotide solutions could also have contributed to the observed difference in T_m.

The effect of the *cs*CPD on the thermal stability of the dsDNA constructs is significant and not unexpected. We observe differences in the T_m of 5−10 °C when undamaged and damaged DNA are compared (Table 2). This is in good agreement with the range of 6−9 °C that has been reported for other dsDNA constructs with 8−12 bp.[20,43−45] For unlabeled DNA, the T_m of the undecamers is 53−54 °C, and the presence of the *cs*CPD decreases it by 5 °C for DNA1 and DNA3 and by 9 °C for DNA2. In DNA1 and DNA3, the *cs*CPD is flanked by GC base pairs on either side, whereas it is flanked by one GC (3′ of *cs*CPD) and one AT (5′ of *cs*CPD) base pair in DNA2. Work by the Stanley group on melting temperatures of *cs*CPD-dsDNA with fluorescent bases has shown that the base pairs on the 5′-side of the CPD, including the 5′-T of the *cs*CPD, are slightly less stable than those on the 3′-side of the CPD.[44,45,47] These results are corroborated by a recent NMR study that shows that the 5′-TA base pair of the CPD is more labile than its 3′-TA base pair.[26] Therefore, it seems that the flanking 5′-TA base pair of the *cs*CPD in DNA2 destabilizes the *cs*CPD-dsDNA slightly more than a flanking GC base pair. This change results in a larger decrease in the T_m of DNA2 in the presence of the *cs*CPD. Because the T_m is the same for DNA1 with the *cs*CPD in the center and DNA3 with the *cs*CPD 1 bp from the 5′-terminus, it appears that end fraying near the *cs*CPD in DNA3 does not result in an additional decrease in the T_m.

Influence of the Location of the CPD on the Binding of Photolyase. The location of the *cs*CPD on the undecamer dsDNA seems to have only a minor effect on the association constant, K_A, of DNA photolyase; K_A is on the order of 2 × 10^6 M^{-1}. Although the *cs*CPD in DNA-3 is only 1 bp from the 5′-terminus, this location does not appear to impede the binding process. All three DNA constructs have the minimal binding unit, i.e., one phosphate 5′ and three phosphates 3′ of the *cs*CPD.[48] The K_A value is significantly lower than what has been published for plasmid DNA (K_A = 4.7−14 × 10^7 M^{-1}), a 43-mer dsDNA (K_A = 10^8 M^{-1}), and poly(dT) (K_A = 4.8 × 10^8 M^{-1}), each containing one or more *cs*CPDs,[36,49,50] while measurements on UV-p$(dT)_2$ and UV-p$(dT)_4$ gave association constants of 1.8 × 10^4 and 4.0 × 10^6 M^{-1}, respectively.[51,52] Our measurements are in excellent agreement with a recent isothermal calorimetry (ITC) experiment, in which the equilibrium constant of binding of photolyase to *cs*CPD-containing poly$(dA{\cdot}dT)_{10}$ was determined to be 1.1 × 10^6 M^{-1} at 17 °C compared to our value of 2 × 10^6 M^{-1} at 15 °C.[24] Our fluorescence method is validated because we obtain virtually the same binding constant with our TET-labeled DNA as that obtained from unlabeled DNA via ITC. The discrepancy between our value and those in the earlier literature has been

DOI: 10.1021/acs.biochem.5b00927
Biochemistry 2015, 54, 6176−6185

Table 3. Equilibrium Association Constants and Association and Dissociation Rate Constants of the dsDNA Constructs Used in This Study

sequence	K_A ($\times 10^6$ M^{-1})	$k_{on,fast}$ ($\times 10^5$ M^{-1} s^{-1})	$k_{on,slow}$ ($\times 10^4$ M^{-1} s^{-1})	k_{off} ($\times 10^{-2}$ s^{-1})[a]
5′-GCAAGTTGGAG-3′ 3′-CGTTCAACCTC-5′	3.2 ± 0.4	2.5 ± 0.4	0.5−1.4	7.8 ± 2.2
5′-CGATTGGAGAG-3′ 3′-GCTAACCTCTC-5′	1.9 ± 0.3	−	2.3 ± 0.3	1.2 ± 0.3
5′-GTTGGAGAGAC-3′ 3′-CAACCTCTCTG-5′	2.2 ± 0.3	2.4 ± 0.3	0.3−2.1	11 ± 3

[a]Calculated by using the dominant rate constant; $k_{off} = k_{on}/K_A$.

discussed in detail by one of us,[24] and we will not elaborate further here.

Given the kinetic traces shown in Figure 3, the position of the *cs*CPD seems to have a significant effect on the rate of binding of DNA photolyase. In DNA1 and DNA3, the binding kinetics show both a fast phase and a slow phase, with the fast phase more dominant in DNA3 (≥85%) than in DNA1 (≈64%). The rate constant associated with the fast phase is ~2.5 × 10^5 M^{-1} s^{-1} in both DNA1 and DNA3, and the slow phase is from 0.03 to 0.21 × 10^5 M^{-1} s^{-1}. The binding kinetics of DNA2 has only a slow phase of 0.23 × 10^5 M^{-1} s^{-1}, slightly faster than that observed for the slow phase in DNA1 and DNA3.

The kinetics of the binding is monitored by the fluorescence of the TET fluorophore. The steady-state data (Figure 2) clearly show quenching of this emission upon protein binding to the DNA molecule, because of RET. The observation of two phases in our data indicates that we may have a complicating factor to consider; we may be detecting a steric effect due to the bulky fluorophore. Therefore, the observation of two rate constants appears to reflect two separate processes: a fast-phase unhindered binding step to photolyase and a slow step due to interference from the TET fluorophore. Our hypothesis is that the *cs*CPD and the fluorophore are aligned in DNA2 in such a way that the fluorophore creates maximal steric interference with photolyase binding and only the slow phase is observed. When the *cs*CPD is moved 2 bp either to the center of the DNA (DNA1) or to the terminus of the DNA (DNA3), the position of the *cs*CPD rotates by approximately 72° and −72° with respect to the fluorophore, respectively, due to the helical nature of dsDNA. This rotation reduces the probability of steric interference of the fluorophore upon binding of photolyase to the *cs*CPD. The observation that the slow phase is much smaller when photolyase binds to DNA3 than to DNA1 supports this hypothesis. In DNA3, the *cs*CPD is farther removed (4 bp, ~13 Å) from the TET fluorophore than in DNA1. The increased distance between the *cs*CPD and TET in DNA3 most likely results in less steric interference of TET during binding, which then translates into a much smaller contribution of the slow phase to the binding kinetics of photolyase and DNA3. Therefore, fluorescent probes can be used to monitor the binding of photolyase to *cs*CPD-DNA, but one has to pay careful attention to possible steric interference of the fluorophore in the binding process. In addition, the observation that K_A is independent of *cs*CPD location also suggests that the photolyase−substrate dissociation rate is slower with DNA2 than with DNA1 and DNA3. The dissociation rates have been calculated from $k_{off} = k_{on}/K_A$ and are listed in Table 3. Apparently, the fluorophore not only slows the formation of the photolyase−substrate complex in the case of DNA2 but also slows the dissociation of the complex.

Only two rate constants, both obtained by indirect measurements, for the binding of photolyase to *cs*CPD-DNA have been reported in the literature. In 1970, Harm reported rate constants of 3.1 × 10^5 M^{-1} s^{-1} (5 °C), 1.1 × 10^6 M^{-1} s^{-1} (23 °C), and 2.1 × 10^6 M^{-1} s^{-1} (37 °C) for *in vivo* experiments.[35] Sancar and co-workers determined binding rate constants of 1.4 × 10^6 and 4.2 × 10^6 M^{-1} s^{-1} at 25 °C for photolyase binding to CPD-containing plasmid DNA.[36] From Harm's work, one can calculate an activation energy of 46 kJ/mol for formation of the enzyme−substrate complex. Using the Arrhenius equation with this activation energy, we calculate the rate constant at 15 °C to be 6.5 × 10^5 M^{-1} s^{-1} for Harm's data and 7.3 × 10^5 to 2.2 × 10^6 M^{-1} s^{-1} for Sancar's data.

Our work shows that photolyase binds to the double-stranded undecamer *cs*CPD-DNA constructs with rate constants that are 2.5−9-fold smaller at 15 °C than those reported for *in vivo* cellular and *in vitro* plasmid DNA studies. It is possible that this reflects a real difference in the binding kinetics of photolyase due to the length of the dsDNA. However, in the earlier work, the binding rate constants were determined indirectly, so some assumptions and estimates to extract the binding rate constants from the experimental data were required; these assumptions introduce some uncertainties into the earlier results. However, it should be noted that neither we nor Sancar finds evidence for binding rate constants on the order of 10^8 M^{-1} s^{-1} as has been determined for other DNA-repair systems. Now that we have a direct way to measure the binding rates of photolyase to its substrate, we can design experiments to investigate inconsistencies with earlier work.

Implications for the Mechanism of CPD Recognition by DNA Photolyase. We determined a rate constant of 2.5 × 10^5 M^{-1} s^{-1} for *E. coli* photolyase binding to the site-specific CPD lesion on dsDNA. This rate constant is significantly smaller than what has been reported in the literature for both sequence-specific and other site-specific DNA binding proteins. For example, the sequence-specific Lac repressor has a binding rate constant of approximately 10^8−10^9 M^{-1} s^{-1} at physiological ionic strengths.[29,30] The site-specific DNA binding enzymes uracil DNA glycosylase (UDG) and DNA methyltransferase M.*Eco*RI bind to their target with rate constants of 2−4 × 10^8 and 1.7−5.0 × 10^7 M^{-1} s^{-1}, respectively, while *Xenopus* XPA binds to a fluorescein-labeled site with a rate constant of 9.0 × 10^8 M^{-1} s^{-1}.[31−34] In general, these large rate constants are attributed to diffusion-controlled nonspecific binding of the protein to DNA followed by one-dimensional facilitated diffusion through sliding, hopping, and/or jumping of the protein in the proximity of and along the DNA to locate and bind to the target sequence or site.[27,28] On the basis of their photolyase binding studies, Sancar and co-workers estimated a ratio of specific to nonspecific binding of photolyase of 2 × 10^5, and they calculated that electrostatic

DOI: 10.1021/acs.biochem.5b00927
Biochemistry 2015, 54, 6176−6185

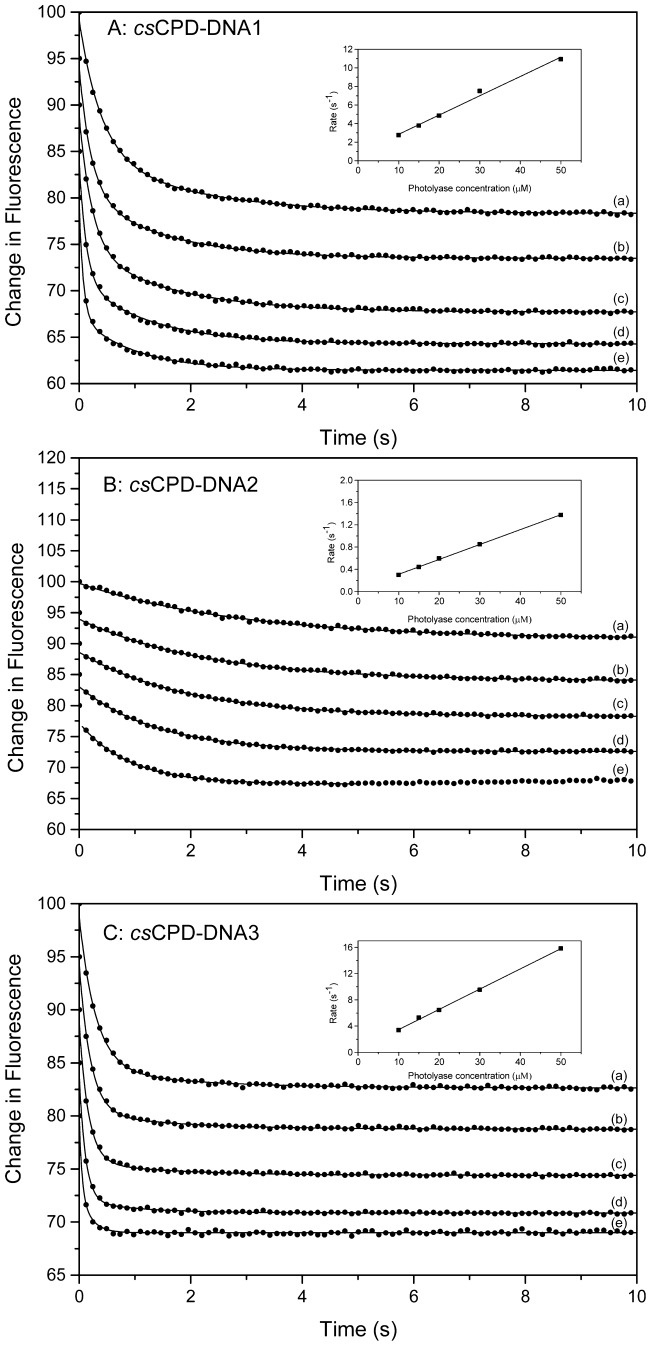

Figure 3. Fluorescence stopped-flow kinetic traces of DNA photolyase binding to (A) *cs*CPD-DNA1, (B) *cs*CPD-DNA2, and (C) *cs*CPD-DNA3. The final concentrations in the mixing cell are 1.0 μM csCPD-DNA and (a) 10, (b) 15, (c) 20, (d) 30, and (e) 50 μM photolyase. For the clarity of the fit (—) to the data (●), only every other 25th data point is shown. The inset of each graph shows the photolyase concentration dependence of the rate (■), and the binding rate constant is the slope of the linear fit (—) to the data.

interactions contributed to only 10% of the overall binding energy.[36] Thus, they concluded that photolyase finds its target through a three-dimensional diffusion-controlled search and argued against contributions from one-dimensional or facilitated diffusion as used by the DNA-repair proteins mentioned above.

The decrease of 100−4000 in the binding rate constant indicates that photolyase must use a significantly different approach to damage recognition than other DNA-repair systems studied. Photolyase and the undecamer dsDNA will have similar three-dimensional diffusion coefficients and, therefore, a diffusional collision rate constant similar to those of other DNA-repair systems.[29−34] Data from other protein−DNA-repair systems are interpreted to show that the protein binds nonspecifically to the DNA and, then, uses sliding, hopping, and/or jumping to find its target sequence or site.[27,28] The target site can be located either by the enzyme flipping the target base out of the duplex DNA or by the enzyme recognizing the extrahelical target. In the case of the photolyase system, the presence of CPD bends and unwinds the dsDNA near the site of the lesion and weakens the 5′-TA base pair and, to a lesser extent, the 3′-TA base pair in the CPD.[20,21,26,44,45,47] Despite obvious structural and, presumably, electrostatic changes near the CPD, photolyase apparently fails to locate the intrahelical CPD through facilitated diffusion after initial three-dimensional diffusion-controlled nonspecific binding to DNA. The recent ITC study has confirmed that nonspecific binding by photolyase to single-stranded DNA is weak ($K_A \leq 200\ M^{-1}$) and that electrostatic contributions of photolyase binding to the CPD are between 5 and 12% of the overall binding energy.[24] This is in line with a reduced role, if any, for facilitated diffusion as pointed out by Sancar.[36]

The comparison with other systems suggests that photolyase may not recognize an intrahelical CPD but only an extrahelical CPD. Such a recognition mechanism has been proposed on the basis of computational studies and ITC experiments.[24,25] If photolyase recognizes only the extrahelical CPD during a three-dimensional diffusion-controlled search, the rate constant for this process is given by

$$k_{CPD} = K_{flip} k_{diffusion} \quad (1)$$

where k_{CPD} is the binding rate constant of photolyase, K_{flip} is the equilibrium constant for spontaneous flipping of the CPD into an extrahelical position, and $k_{diffusion}$ is the three-dimensional diffusional collision rate constant. For proteins of a size similar to that of photolyase and interacting with short dsDNA, $k_{diffusion} \approx k_{on} = 1.7 \times 10^7$ to $9.0 \times 10^8\ M^{-1}\ s^{-1}$.[29−34] Therefore, using a k_{CPD} of $2.5 \times 10^5\ M^{-1}\ s^{-1}$, we predict that K_{flip} values of 1.5×10^{-2} to 2.8×10^{-4} would be sufficient to support a purely three-dimensional search.

A computational study estimated K_{flip} to be on the order of 5×10^{-5}, and this result was interpreted in favor of photolyase recognizing an extrahelical *cs*CPD.[25] Experimentally, two NMR studies used imino proton exchange reactions to study base pair opening in *cs*CPD-containing dsDNA. In one study, αK_{open}, the apparent equilibrium constant for base pair opening, was found to increase from 6.5×10^{-6} for the 5′-T·A in undamaged dsDNA to 8.9×10^{-6} for 5′-T·A of the CPD, and $\alpha K_{open} = 3.1 \times 10^{-6}$ for 3′-T·A in undamaged dsDNA.[53] The parameter α depends on the base catalyst that is used for the imino proton exchange measurements, and $\alpha \leq 1$,[54] where $K_{open} \geq \alpha K_{open}$. In a second study, it was found that K_{open} increased from 8×10^{-7} for the 5′-TA in undamaged dsDNA to 2×10^{-4} for 5′-TA of the CPD, and it increased from 2.5×10^{-6} for the 3′-TA in undamaged dsDNA to 3×10^{-5} for 3′-TA of the CPD.[26] In that study, α was assumed to be equal to unity for ammonia as the base catalyst. It was also pointed out that the pK_a values of the CPD imino protons are not known and that an increase in their pK_a by 1 pH unit due to loss of aromaticity upon CPD formation would increase K_{open} by a factor of 10 to 2×10^{-3}

DOI: 10.1021/acs.biochem.5b00927
Biochemistry 2015, 54, 6176−6185

and 3×10^{-4} for the 5′-TA and 3′-TA base pairs of the CPD, respectively.

The authors of the NMR study argue against spontaneous flipping of the CPD into an extrahelical position and suggest that K_{open} reflects flipping of the adenosine bases opposite of the CPD that gives rise to CPD imino proton exchange.[26] However, the K_{open} of the 5′-TA falls within our predicted range for K_{flip}, and, if the pK_a of the imino protons would be higher in the CPD than in thymidine monomers, K_{open} values for both 5′-TA and 3′-TA would fall within the range that would support recognition of an extrahelical CPD by photolyase, assuming that K_{open} reflects K_{flip}. The preponderance of the experimental data supports the hypothesis that photolyase recognizes an extrahelical CPD.

The notion that photolyase is significantly slower than other DNA-repair systems is not at odds with its efficient repair of *cs*CPD-DNA. After photolyase has found and bound to a *cs*CPD, it has to absorb a photon of the correct energy to catalyze the monomerization of the dimerized thymidines, which seems to be the rate-limiting step. In earlier work, we concluded that this is not a problem because substrate binding stabilizes the active form of the enzyme under physiological conditions.[55] Therefore, the enzyme is not optimized for finding of the *cs*CPD but for maintaining the enzyme−substrate complex as well as the active form of the enzyme until absorption of a blue-light photon has occurred to catalyze the repair.

CONCLUSION

Our results show that dsDNA can be labeled with a fluorophore to study the binding of photolyase to *cs*CPD-containing DNA. However, one has to pay careful attention to the location of the fluorophore with respect to the *cs*CPD lesion to avoid steric interference from the fluorophore during the binding process. Neither the location of the *cs*CPD on the undecamer dsDNA nor the presence of the fluorophore has any significant effect on the thermal stability of the DNA as determined by its melting temperature.

When we omit the data that appear to be affected by steric interference from the fluorophore, we find that the association constant of photolyase is independent of the location of the *cs*CPD whether in the center or at the terminus of the undecamer DNA. The K_a value of $\sim 2 \times 10^6$ M^{-1} is in good agreement with the literature for similar substrates. In contrast, the kinetics of binding of photolyase to the *cs*CPD undecamer DNA is sensitive to the relative position of the *cs*CPD with respect to the fluorophore. For the binding rate constant, we find a k_{on} of $\sim 2.5 \times 10^5$ M^{-1} s^{-1}, which is slightly slower than rate constants that were obtained through indirect measurements *in vivo* in *E. coli* cells and *in vitro* with plasmid DNA.[35,36] Most importantly, the photolyase binding rate constant is 100−4000 times slower than that for other DNA-repair systems. These other proteins bind nonspecifically to DNA with a rate constant that is limited by three-dimensional diffusion coefficients and rapidly locate their target through facilitated diffusion in the form of sliding, hopping, and/or jumping along the DNA without completely dissociating. It appears that photolyase does not follow such a search process and instead may rely on a three-dimensional search for an extrahelical *cs*CPD, which spontaneously flips in and out of the double helix. Experiments to further test this proposed mechanism are underway.

AUTHOR INFORMATION

Corresponding Author

*Department of Chemistry and Biochemistry, Montclair State University, 1 Normal Ave., Montclair, NJ 07043. E-mail: schelvisj@mail.montclair.edu. Telephone: (973) 655 3301.

Present Address

[§]X.Z.: Moderna Therapeutics, 320 Bent St., Cambridge, MA 02141.

Funding

The research was sponsored by National Science Foundation Grants MCB 0415611 (J.P.M.S.) and 0742122 (J.P.M.S.).

Notes

The authors declare no competing financial interest.

ACKNOWLEDGMENTS

We acknowledge Drs. Richard Magliozzo and Xiangbo Zhao at Brooklyn College for their help with the stopped-flow experiments and for providing access to the stopped-flow apparatus. Part of the research was conducted at New York University (X.Z. and J.P.M.S.) and at Lafayette College (Y.M.G.).

REFERENCES

(1) Sancar, A. (2003) Structure and Function of DNA Photolyase and Cryptochrome Blue-Light Photoreceptors. *Chem. Rev. 103*, 2203−2237.

(2) Brettel, K., and Byrdin, M. (2010) Reaction Mechanism of DNA Photolyase. *Curr. Opin. Struct. Biol. 20*, 693−701.

(3) Kneuttinger, A. C., Kashiwazaki, G., Prill, S., Heil, K., Müller, M., and Carell, T. (2014) Formation and Direct Repair of UV-induced Dimeric DNA Pyrimidine Lesions. *Photochem. Photobiol. 90*, 1−14.

(4) Taylor, J.-S. (1994) Unraveling the Molecular Pathway from Sunlight to Skin Cancer. *Acc. Chem. Res. 27*, 76−82.

(5) Mouret, S., Baudouin, C., Charveron, M., Favier, A., Cadet, J., and Douki, T. (2006) Cyclobutane pyrimidine dimers are predominant DNA lesions in whole human skin exposed to UVA radiation. *Proc. Natl. Acad. Sci. U. S. A. 103*, 13765−13770.

(6) MacFarlane, A. W., IV, and Stanley, R. J. (2003) *Cis-Syn* Thymidine Dimer Repair by DNA Photolyase in Real Time. *Biochemistry 42*, 8558−8568.

(7) Kao, Y.-T., Saxena, C., Wang, L., Sancar, A., and Zhong, D. (2005) Direct observation of thymine dimer repair in DNA photolyase. *Proc. Natl. Acad. Sci. U. S. A. 102*, 16128−16132.

(8) Thiagarajan, V., Byrdin, M., Eker, A. P. M., Muller, P., and Brettel, K. (2011) Kinetics of cyclobutane thymine dimer splitting by DNA photolyase directly monitored in the UV. *Proc. Natl. Acad. Sci. U. S. A. 108*, 9402−9407.

(9) Park, H.-W., Kim, S.-T., Sancar, A., and Deisenhofer, J. (1995) Crystal structure of DNA photolyase from Escherichia coli. *Science 268*, 1866−1872.

(10) Vande Berg, B. J., and Sancar, G. B. (1998) Evidence for Dinucleotide Flipping by DNA Photolyase. *J. Biol. Chem. 273*, 20276−20282.

(11) Sanders, D. B., and Wiest, O. (1999) A Model for the Enzyme Substrate Complex of DNA Photolyase and Photodamaged DNA. *J. Am. Chem. Soc. 121*, 5127−5134.

(12) Antony, J., Medvedev, M., and Stuchebrukhov, A. A. (2000) Theoretical Study of Electron Transfer between the Photolyase Catalytic Cofactor FADH- and DNA Thymine Dimer. *J. Am. Chem. Soc. 122*, 1057−1065.

(13) MacFarlane, A. W., IV, and Stanley, R. J. (2001) Evidence of Powerful Substrate Electric Fields in DNA Photolyase: Implications for Thymidine Dimer Repair. *Biochemistry 40*, 15203−15214.

(14) Christine, K. S., MacFarlane, A. W., Yang, K., and Stanley, R. J. (2002) Cyclobutanepyrimidine Dimer Base Flipping by DNA Photolyase. *J. Biol. Chem. 277*, 38339−38344.

DOI: 10.1021/acs.biochem.5b00927
Biochemistry 2015, 54, 6176−6185

(15) Torizawa, T., Ueda, T., Kuramitsu, S., Hitomi, K., Todo, T., Iwai, S., Morikawa, K., and Shimada, I. (2004) Investigation of the Cyclobutane Pyrimidine Dimer (CPD) Photolyase DNA Recognition Mechanism by NMR Analysis. *J. Biol. Chem. 279*, 32950−32956.
(16) Schelvis, J. P. M., Ramsey, M., Sokolova, O., Tavares, C., Cecala, C., Connell, K., Wagner, S., and Gindt, Y. M. (2003) Resonance Raman and UV-Vis Spectroscopic Characterization of FADH• in the Complex of Photolyase with UV-Damaged DNA. *J. Phys. Chem. B 107*, 12352−12362.
(17) Kapetanaki, S. M., Ramsey, M., Gindt, Y. M., and Schelvis, J. P. M. (2004) Substrate Electric Dipole Moment Exerts a pH-Dependent Effect on Electron Transfer in Escherichia coli Photolyase. *J. Am. Chem. Soc. 126*, 6214−6215.
(18) Murphy, A. K., Tammaro, M., Cortazar, F., Gindt, Y. M., and Schelvis, J. P. M. (2008) Effect of Cyclobutane Cytidine Dimer on the Properties of Escherichia coli DNA Photolyase. *J. Phys. Chem. B 112*, 15217−15226.
(19) Mees, A., Klar, T., Gnau, P., Hennecke, U., Eker, A. P. M., Carell, T., and Essen, L.-O. (2004) Crystal Structure of a Photolyase Bound to a CPD-Like DNA Lesion After *in situ* Repair. *Science 306*, 1789−1793.
(20) McAteer, K., Jing, Y., Kao, J., Taylor, J.-S., and Kennedy, M. A. (1998) Solution-state Structure of a DNA Dodecamer Duplex Containing a *Cis-Syn* Thymine Cyclobutane Dimer, the Major UV Photoproduct of DNA. *J. Mol. Biol. 282*, 1013−1032.
(21) Park, H., Zhang, K., Ren, Y., Nadji, S., Sinha, N., Taylor, J.-S., and Kang, C. (2002) Crystal structure of a DNA decamer containing a *cis-syn* thymine dimer. *Proc. Natl. Acad. Sci. U. S. A. 99*, 15965−15970.
(22) Roberts, R. J., and Cheng, D. (1998) Base Flipping. *Annu. Rev. Biochem. 67*, 181−198.
(23) Stivers, J. T., and Jiang, Y. L. (2003) A Mechanistic Perspective on the Chemistry of DNA Repair Glycosylases. *Chem. Rev. 103*, 2729−2759.
(24) Wilson, T. J., Crystal, M. A., Rohrbaugh, M. C., Sokolowsky, K. P., and Gindt, Y. M. (2011) Evidence from Thermodynamics that DNA Photolyase Recognizes a Solvent-Exposed CPD Lesion. *J. Phys. Chem. B 115*, 13746−13754.
(25) O'Neil, L. L., Grossfield, A., and Wiest, O. (2007) Base Flipping of the Thymine Dimer in Duplex DNA. *J. Phys. Chem. B 111*, 11843−11849.
(26) Wenke, B. B., Huiting, L. N., Frankel, E. B., Lane, B. F., and Núñez (2013) Base Pair Opening in a Deoxynucleotide Duplex Containing a *cis-syn* Thymine Cyclobutane Dimer Lesion. *Biochemistry 52*, 9275−9285.
(27) Halford, S. E. (2009) An End to 40 Years of Mistakes in DNA-Protein Association Kinetics? *Biochem. Soc. Trans. 37*, 343−348.
(28) Friedman, J. I., and Stivers, J. T. (2010) Detection of Damaged DNA Bases by DNA Glycosylase Enzymes. *Biochemistry 49*, 4957−4967.
(29) Barkley, M. D. (1981) Salt Dependence of the Kinetics of the *lac* Repressor-Operator Interaction: Role of Nonoperator Deoxyribonucleic Acid in the Association Reaction. *Biochemistry 20*, 3833−3842.
(30) Winter, R. B., Berg, O. G., and von Hippel, P. H. (1981) Diffusion-Driven Mechanisms of Protein Translocation on Nucleic Acids 3. The *Escherichia coli lac* Repressor-Operator Interaction: Kinetic Measurements and Conclusions. *Biochemistry 20*, 6961−6977.
(31) Hopkins, B. B., and Reich, N. O. (2004) Simultaneous DNA Binding, Bending, and Base Flipping. *J. Biol. Chem. 279*, 37049−37060.
(32) Krosky, D. J., Song, F., and Stivers, J. T. (2005) The Origins of High-Affinity Enzyme Binding to an Extrahelical DNA Base. *Biochemistry 44*, 5949−5959.
(33) Porecha, R. H., and Stivers, J. T. (2008) Uracil DNA Glycosylase Uses DNA Hopping and Short-Range Sliding to Trap Extrahelical Uracils. *Proc. Natl. Acad. Sci. U. S. A. 105*, 10791−10796.
(34) Iakoucheva, L. M., Walker, R. K., van Houten, B., and Ackerman, E. J. (2002) Equilibrium and Stopped-Flow Kinetic Studies of Fluorescently Labeled DNA Substrates with DNA Repair Proteins XPA and Replication Protein A. *Biochemistry 41*, 131−143.
(35) Harm, W. (1970) Analysis of Photoenzymatic Repair of UV Lesions in DNA by Single Light Flashes. V. Determination of the Reaction Rate Constants in *E. coli* Cells. *Mutat. Res., Fundam. Mol. Mech. Mutagen. 10*, 277−290.
(36) Sancar, G. B., Smith, F. W., Reid, R., Payne, G., Levy, M., and Sancar, A. (1987) Action Mechanism of *Escherichia coli* DNA Photolyase. *J. Biol. Chem. 262*, 478−485.
(37) Gindt, Y. M., Vollenbroek, E., Westphal, K., Sackett, H., Sancar, A., and Babcock, G. T. (1999) Origin of the Transient Electronic Paramagnetic Resonance Signals in DNA Photolyase. *Biochemistry 38*, 3857−3866.
(38) Förster, T. (1948) Zwischenmolekulare Energiewanderung und Fluoreszenz. *Ann. Phys. 437*, 55−75.
(39) Stryer, L., and Haugland, R. P. (1967) Energy Transfer. Spectroscopic Ruler. *Proc. Natl. Acad. Sci. U. S. A. 58*, 719−726.
(40) Wang, B., and Jorns, M. S. (1989) Reconstitution of Escherichia coli DNA Photolyase with Various Folates. *Biochemistry 28*, 1148−1152.
(41) Banerjee, S. K., Christensen, R. B., Lawrence, C. W., and LeClerc, J. E. (1988) Frequency and Spectrum of Mutations Produced by a Single cis-syn Thymine-Thymine Cyclobutane Dimer in a Single-Stranded Vector. *Proc. Natl. Acad. Sci. U. S. A. 85*, 8141−8145.
(42) Cantor, C. R., Warshaw, M. M., and Shapiro, H. (1970) Oligonucleotide Interactions III: Circular Dichroism Studies of the Formation of Deoxyoligonucleotides. *Biopolymers 9*, 1059−1077.
(43) Taylor, J.-S., Garrett, D. S., Brockie, I. R., Svoboda, D. L., and Telser, J. (1990) ^{1}H NMR Assignment and Melting Temperature Study of Cis-Syn and Trans-Syn Thymine Dimer Containing Duplexes of d(CGTATTATGC)•d(GCATAATACG). *Biochemistry 29*, 8858−8866.
(44) Yang, K., and Stanley, R. J. (2006) Differential Distortion of Substrate Occurs When It Binds to DNA Photolyase: A 2-Aminopurine Study. *Biochemistry 45*, 11239−11245.
(45) Yang, K., Matsika, S., and Stanley, R. J. (2007) 6MAP, a Fluorescent Adenine Analogue, Is a Probe of Base Flipping by DNA Photolyase. *J. Phys. Chem. B 111*, 10615−10625.
(46) Nazarenko, I., Pires, R., Lowe, B., Obaidy, M., and Rashtchian, A. (2002) Effect of Primary and Secondary Structure of Oligodeoxyribonucleotides on the Fluorescenct Properties of Conjugated Dyes. *Nucleic Acids Res. 30*, 2089−2195.
(47) Yang, K., and Stanley, R. S. (2008) The Extent of DNA Deformation in DNA Photolyase-Substrate Complexes: A Solution State Fluorescence Study. *Photochem. Photobiol. 84*, 741−749.
(48) Husain, I., Sancar, G. B., Holbrook, S. R., and Sancar, A. (1987) Mechanism of Damage Recognition by *Escherichia coli* DNA Photolyase. *J. Biol. Chem. 262*, 13188−13197.
(49) Husian, I., and Sancar, A. (1987) Binding of E. coli photolyase to a defined substrate containing a single T< > T dimer. *Nucleic Acids Res. 15*, 1109−1120.
(50) Kim, S.-T., and Sancar, A. (1991) Effect of base, pentose, and backbone structures on binding and repair of pyrimidine dimers by Escherichia coli DNA photolyase. *Biochemistry 30*, 8623−30.
(51) Jordan, S. P., and Jorns, M. S. (1988) Evidence for a singlet intermediate in catalysis by Escherichia coli DNA photolyase and evaluation of substrate binding determinants. *Biochemistry 27*, 8915−8923.
(52) Jordan, S. P., Alderfer, J. L., Chanderkar, L. P., and Jorns, M. S. (1989) Reaction of Escherichia coli and yeast photolyases with homogenous short-chain oligonucleotide substrates. *Biochemistry 28*, 8149−8153.
(53) Bang, J., Kang, Y.-M., Park, C.-J., Lee, J.-H., and Choi, B.-S. (2009) Thermodynamics and Kinetics for Base Pair Opening in the DNA Decamer Duplexes Containing Cyclobutane Pyrimidine Dimer. *FEBS Lett. 583*, 2037−2041.
(54) Kochoyan, M., Leroy, J. L., and Guéron, M. (1987) Proton Exchange and Base-pair Lifetimes in a Deoxy-duplex Containing a Purine-Pyrimidine Step and in the Duplex of Inverse Sequence. *J. Mol. Biol. 196*, 599−609.

DOI: 10.1021/acs.biochem.5b00927
Biochemistry 2015, 54, 6176−6185

(55) Gindt, Y. M., Schelvis, J. P. M., Thoren, K. L., and Huang, T. H. (2005) Substrate Binding Modulates the Reduction Potential of DNA Photolyase. *J. Am. Chem. Soc. 127*, 10472−10473.

DOI: 10.1021/acs.biochem.5b00927
Biochemistry 2015, 54, 6176−6185